

PAPER • OPEN ACCESS

Characterization of annatto (*bixa orellana*) peels activated carbon and its application as adsorbent for natural dyes from annatto seeds

To cite this article: Cucun Alep Riyanto 2019 *IOP Conf. Ser.: Mater. Sci. Eng.* **509** 012029

View the [article online](#) for updates and enhancements.

Characterization of annatto (*bixa orellana*) peels activated carbon and its application as adsorbent for natural dyes from annatto seeds

Cucun Alep Riyanto¹

¹ Department of Chemistry, Faculty of Science and Mathematics, Universitas Kristen Satya Wacana, Jalan Diponegoro 52-60, Salatiga, Indonesia
Email: cucun.alep@staff.uksw.edu

Abstract. This study aims to fabricated activated carbon from annatto (*B. orellana*) peels and to apply that as a natural dyes adsorbent from annatto seeds. The fabrication process methods through the physical and chemical activation. The study of adsorption includes the adsorption kinetics and isotherms of natural dyes from annatto seeds using annatto peels activated carbon (APAC). The amount of natural dyes adsorption measured using UV-Vis spectrophotometer with the calculation of impairment of absorbance value. The APAC can be generated from the carbonization process at 400°C for an hour and two-stage activation process (physical and chemical activation) with H₃PO₄ 30% as an activator and the impregnation ratio of 1:4 (w/w) for 24 hours. The APAC has characteristics such as standard activated carbon based on analysis with FTIR spectrophotometer and X-ray Diffractometer. The peak of APAC diffraction was detected at 2theta = 24.081° and 42.858°. The adsorption kinetics of ACAP on annatto seeds extract (ASE) followed the pseudo second-order kinetic model with the rate constant of adsorption is 78.5514 g mg⁻¹ h⁻¹ on 150 minutes for contact time. This adsorption process followed the Elovic isotherm models with multilayer adsorption.

Keywords: activated carbon, adsorption, annatto peel, isotherm, kinetics, natural dyes

1. Introduction

Nowadays the technological developments have entered nanotechnology, utilizing a nanometer size (10⁹m) of materials that can be applied to various aspects, such as chemistry, biology, medicine, materials, and electronics. According to Pari *et al.* [1], the main advantage of nanotechnology is the emergence of new functions of a substance at the nanoscale. Nanotechnology research that has been carried out are nanocomposites, nanocrystals, nanoparticles, nanostructure, nanocatalysts, nanofibers, and nanocarbon. One of the most widely used nanomaterial products is nanocarbon.

In its development, nanocarbon can be used as activated carbon with raw materials that can come from carbonized charcoal. Some of the manufactures of activated carbon has been carried out from cassava peel [2], sawdust of Algaroba wood [3], coffee waste [4], kenaf fibre [5], palm oil fronds [6], Fox peanuts [7], coconut shells [8], kenaf core [9], and tobacco stem [10]. These studies produce activated carbon with several methods, one of them with temperature activation and acid activation (H₃PO₄). From these research, all of the activated carbon product was obtained from natural sources such as plants.

The annatto plant (*Bixa orellana*) is one of the plants that live in the tropics country, one of which is Indonesia. One of the benefits of this plant is its seeds, which are as natural dyes for clothing such as



cotton and wool [11]. The annatto seeds are known to contain bixin and nor-bixin compounds [12, 13]. Furthermore, [14] researched the natural dyes of annatto seeds and applied that in belts.

Based on previous researches, the annatto plant are more used as natural dye agents from its seeds, but the annatto peels have not been used. Therefore, this research will use the annatto peels as a source of raw material to produce activated carbon. In addition, the activated carbon will be tested as an adsorbent for natural dyes from annatto seeds based on the study of adsorption kinetics and isotherms.

2. Methodology

2.1. Material and Equipment

The annatto peels (*B. orellana*) obtained from Perpustakaan Notohamidjojo UKSW. The material used include H_3PO_4 85% ($\rho=1.7\text{g/cm}^3$), NaOH, methanol, chloroform, and HNO_3 65%. All reagents that used are pro-analysis grade from E-Merck Germany. The tools used in this study include an analytical balance of 0.01g (OHAUS TAJ 601), analytical balance with 0.1 mg accuracy (OHAUS PA 214), moisture analyser (OHAUS MB 25), pH meter (HANNA HI 9812), furnace (Vulcan A-550), reflux device, and sets of Buchner vacuum pump. The instruments used were Infrared Spectrophotometer (FT-IR, Shimadzu Prestige 21), X-Ray Diffractometer (XRD, Rigaku Multiflex 2kW), and UV-VIS Spectrophotometer (Optizen UV 2120).

2.2. Preparation of annatto peel ([15] with modified)

The annatto peels were washed with hot distilled water and cut into pieces and dried ($T=75^\circ\text{C}$). After drying, the sample is smoothed and sieved with a 60 mesh sieve.

2.3. Extraction of annatto seed dyes ([14] with modified)

The annatto seeds were crushed (5 g) and shaken with 100 mL of distilled water then refluxed for 60 minutes ($T=80^\circ\text{C}$). During the reflux process, the natural dye will be produced. After that, the extract solution was filtered with filter paper to obtain an annatto seed extract (ASE).

2.4. Sample carbonization ([9] with modified)

The sample was carbonized at furnace ($T=400^\circ\text{C}$) for an hour. Carbon was impregnated with 30% orthophosphoric acid (H_3PO_4) and the impregnation ratio 1:4 (w/w) for 24 hours. After that, the sample was filtered with a Buchner vacuum pump and dehydrated overnight in an oven at 105°C . The dried sample was then pyrolyzed with activated for 1 hour ($T=500^\circ\text{C}$) and washed with NaOH 1M then rinsed with distilled water until pH of 6-7. The activated carbon was then dried in an oven at $T=105^\circ\text{C}$ at 24 hours.

2.5. Sample purification ([16] with modified)

Activated carbon was refluxed for 4 hours with a solvent of 65% HNO_3 ($T=100^\circ\text{C}$) then washed with distilled water to pH of 6-7. After that, it is dried overnight in an oven ($T=110^\circ\text{C}$). Activated carbon that has dried and then mashed and sieved with a 60 mesh size sieve.

2.6. Sample characterization

The analyse of the functional group of annatto peels activated carbon (APAC) observed with an Infrared Spectrophotometer at a wavenumber of $4000\text{--}400\text{ cm}^{-1}$. Crystallinity properties from the APAC analysed by X-ray Diffractometer.

2.7. Application of natural dyes adsorption with activated carbon

The adsorption process was carried out with variation mass of APAC (0, 20, 40, 60, 80, 100, 120, 140, and 160 mg) in 20 mL of ASE solution for 0, 30, 60, 90, 120, 150, 180, 210, and 240 minutes [15-17]. The adsorbed natural dyes content was determined by measuring the absorbance of the solution using a UV-Vis spectrophotometer ($\lambda_{\text{maks}}=487\text{ nm}$) [14].

3. Results and Discussion

3.1. Characterization of Activated Carbon

The FTIR results of carbonization and activation of annatto peel with impregnation ratio 1:4 (w/w) of 30% orthophosphoric acid (H_3PO_4) are presented in Fig 1.

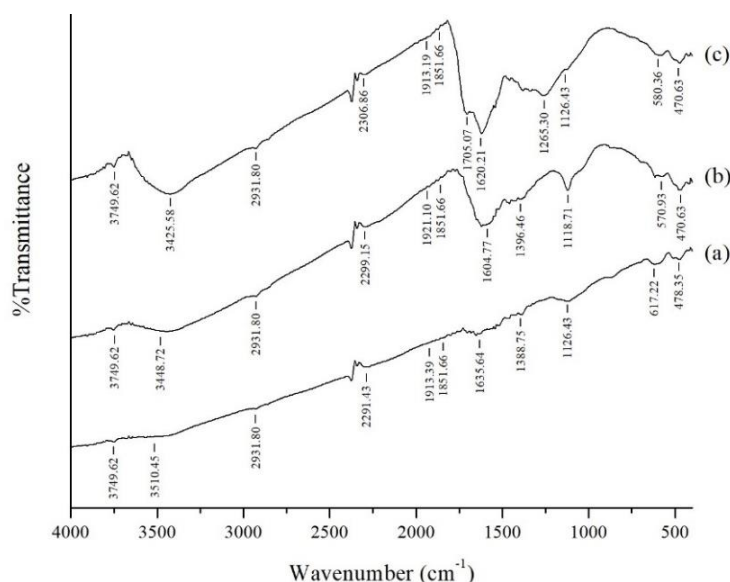


Figure 1. FT-IR spectra of standard activated carbon (a); raw AP (b); and ACAP (c).

Fig 1 shows the similarity of detection for absorption bands in wavenumber in each test sample. In Fig 1(b-c), there is an absorption band at 3425.58 cm^{-1} and 3448.72 cm^{-1} representing stretching vibration of O-H in hydroxyl groups. The band at 2931.80 cm^{-1} attributed to C-H vibration, also at $1635\text{--}1627\text{ cm}^{-1}$ that represented the stretching of C=O [18]. The new absorption band at 1705.07 cm^{-1} indicated the vibration of P=O [21]. The presence of P=O groups is due to the use of H_3PO_4 as an activator in the fabrication of activated carbon. Based on the FT-IR spectra, we can know that the APAC spectra corresponds to the standard activated carbon spectra.

From the FT-IR spectra results, the characterization was continued with an X-Ray Diffractometer. Characterization results are presented in Fig 2.

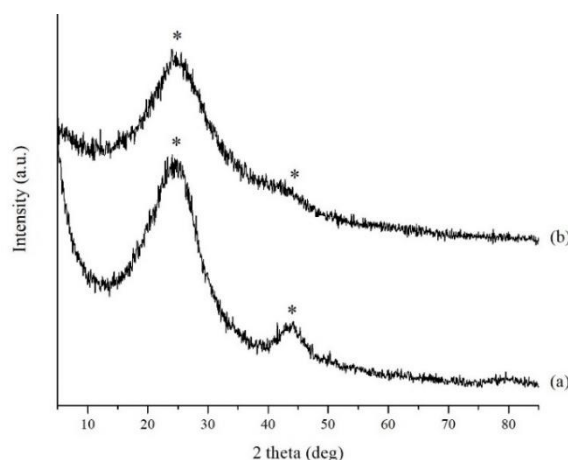


Figure 2. X-Ray diffractogram of standard activated carbon (a) and ACAP (b).

Based on Fig 2a, the diffraction peaks look quite clear at $2\text{-theta} = 24.059^\circ$ and 44.222° for standard activated carbon [9, 19]. When compared to Fig 2b, the diffraction peaks for APAC correspond to diffraction peaks on standard activated carbon at $2\text{-theta} = 24.081^\circ$ and 42.858° . The suitability of the diffraction peak shows that the fabrication of activated carbon from annatto peel has been done successfully. The diffraction peak at $2\text{-theta} = 42.858^\circ$ which is not clearly seen because there are still some impurities in the sample so that further purification processes are needed.

3.2. Adsorption Study

The results of ACAP obtained were then tested as adsorbents of natural dyes from the extracts of annatto seeds (ASE). In this research, the study of ASE adsorption by ACAP was determined from adsorption kinetics and isotherms. The adsorption kinetics of ASE by ACAP was determined using the pseudo second-order model, Elovich model, and intraparticle diffusion model [17]. These kinetic equations are given as follow:

Pseudo second-order kinetic model:

$$\frac{t}{q_t} = \frac{1}{k_2 q_e^2} + \frac{1}{q_e} t \quad (1)$$

where k_2 is the pseudo second-order rate constant of adsorption ($\text{g mg}^{-1} \text{h}^{-1}$). The magnitudes of q_e and k_2 are determined from the slope and intercept of the plot of t/q_t versus t .

Elovic kinetic model:

$$q_t = \frac{1}{\beta} \ln \alpha \beta + \frac{1}{\beta} \ln t \quad (2)$$

where α is the initial adsorption rate ($\text{mg g}^{-1} \text{h}^{-1}$). The plot of q_t against $\ln t$ should obtain a linear relationship with a slope of $(1/\beta)$ and intercept of $(1/\beta) \ln \alpha \beta$.

Intraparticle diffusion kinetic model:

$$q_t = K_{\text{dif}} t^{1/2} + I \quad (3)$$

where I (mg g^{-1}) is the intercept and K_{dif} is the intraparticle diffusion rate constant ($\text{mg g}^{-1} \text{min}^{-1/2}$). The value of q_t is linearly correlated with $t^{1/2}$, and the K_{dif} can be calculated directly from the slope of the plot. The results of adsorption kinetics presented in Fig 3.

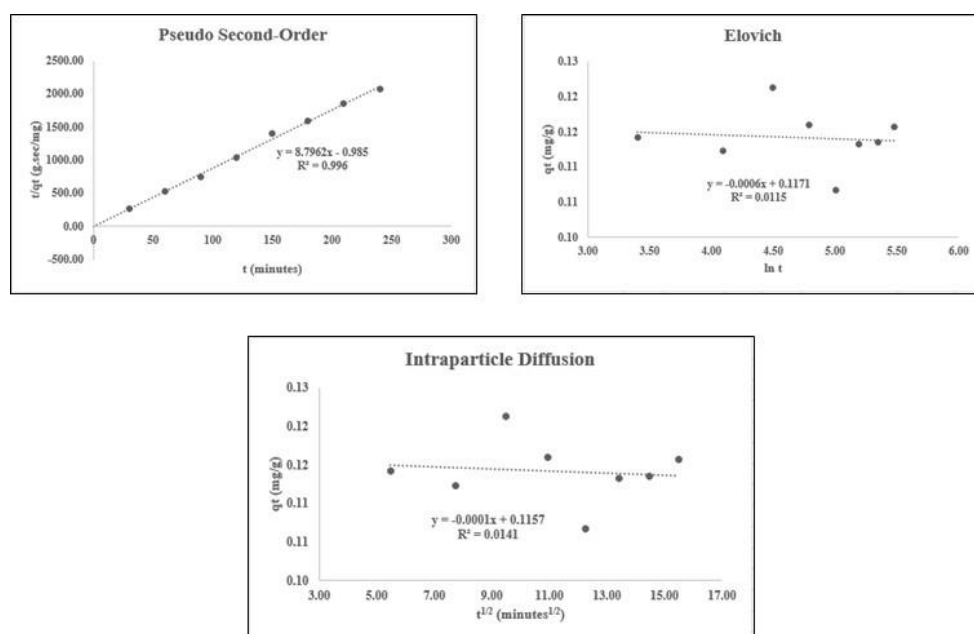


Figure 3. Adsorption kinetics models of adsorption ASE by ACAP.

Based on the results of the adsorption kinetics modelling (Fig. 3), the R^2 value for pseudo second-order kinetics, Elovich, and intraparticle diffusion was obtained at 0.996, 0.0115, and 0.0141, respectively. From that results, the modelling of the pseudo second-order was plotted as APAC adsorption modelling for the ASE with the rate constant of adsorption is $78.5514 \text{ g mg}^{-1} \text{ h}^{-1}$. This modelling was chosen because the R^2 value obtained was more than 0.9000 [19]. From this modelling, the best results of contact time for adsorption ASE by APAC was obtained for 150 minutes with the highest difference in absorbance is 0.073 (Fig. 4).

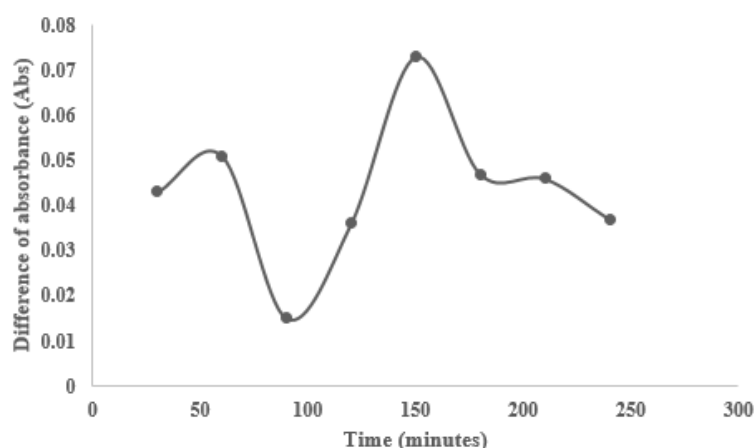


Figure 4. Contact time for adsorption of ASE by APAC.

After the results of the adsorption kinetics, the study of adsorption isotherms was determined by varying the weight of the ACAP adsorbent used for ASE adsorption during 150 minutes' contact times. In this research, the adsorption isotherm models used are the Langmuir isotherm model, Freundlich isotherm model, Jovanovich isotherm model, Elovich isotherm model, and Redlich-Peterson isotherm model [23]. These isotherm equations are given as follow:

Langmuir isotherm model:

$$\frac{C_e}{q_e} = \frac{1}{q_m K_L} + \frac{C_e}{q_m} \quad (4)$$

where C_e is a concentration of adsorbate at equilibrium (mg g^{-1}). K_L is Langmuir constant that related to adsorption capacity (mg g^{-1}), which can be correlated with the variation of the suitable area and porosity of the adsorbent.

Freundlich isotherm model:

$$\log q_e = \log K_F + \frac{1}{n} \log C_e \quad (5)$$

where K_F is adsorption capacity (L/mg) and $1/n$ is adsorption intensity, it also indicates the relative distribution of the energy and the heterogeneity of the adsorbate sites.

Jovanovich isotherm model:

$$\ln q_e = \ln q_{\max} - K_J C_e \quad (6)$$

where q_e is an amount of adsorbate in the adsorbent at equilibrium (mg g^{-1}), q_{\max} is the maximum uptake of adsorbate can be calculated from the plot of $\ln q_e$ versus C_e , and K_J is Jovanovic constant.

Elovich isotherm model:

$$\ln \frac{q_e}{C_e} = \ln K_E q_m - \frac{q_e}{q_m} \quad (7)$$

Elovich maximum adsorption capacity and Elovich constant can be calculated from the slope and intercept of the plot of $\ln \frac{q_e}{C_e}$ versus q_e .

Redlich-Peterson isotherm model:

$$\ln \frac{C_e}{q_e} = \beta \ln C_e - \ln A \quad (8)$$

The Redlich-Peterson constants can be determined from the plot of $\ln C_e/q_e$ versus $\ln C_e$, where β is the slope, and A is intercept. The results of adsorption isotherm presented in Fig 5.

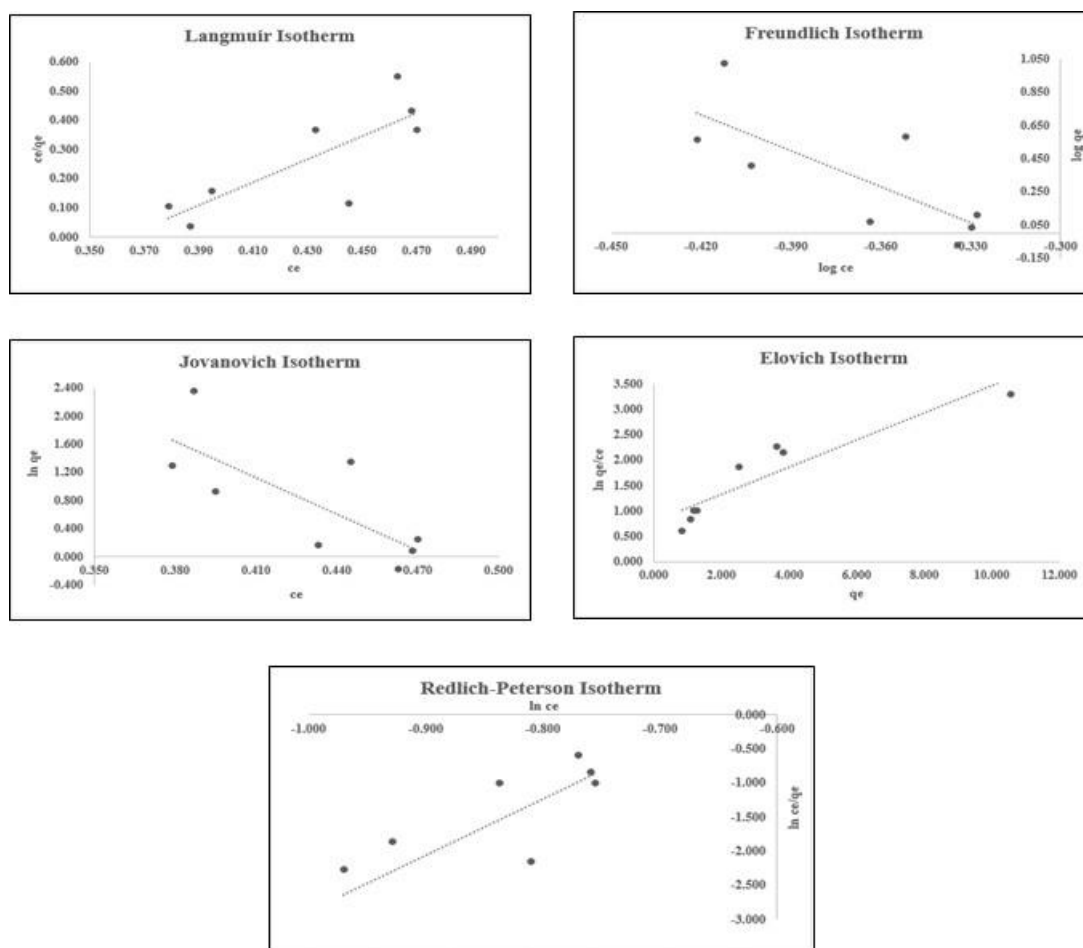


Figure 5. Adsorption isotherm modelling for the adsorption of ASE by APAC.

From the results of the adsorption isotherm modelling plot for the adsorption of ASE by APAC, we can determine the isotherm parameters using the original form of the isotherm equation. The detailed parameters of the five models presented in Table 1.

Based on the detail results from Fig 5 and Table 1, the adsorption isotherm for ASE by APAC tend to follow Elovich isotherm because this model has the highest linearity compared to other models of 0.8556. The Elovich isotherm model assumed that the adsorption sites increase exponentially with adsorption, this implies multilayer adsorption [20]. So, we can assume that the surface of the ACAP adsorbent consists of multilayer active sites.

Table 1. Isotherm parameters for the adsorption of ASE by APAC.

Isotherm	Constants		Linearity
Langmuir	q_m (mg/g)	K_L (L/mg)	R^2
	0.2527	2.7565	0.6512
Freundlich	n	K_F (L/g)	R^2
	7.2564	2.3316	0.5726
Jovanovich	q_{max} (mg/g)	K_J (L/g)	R^2
	3,449.898	17.129	0.5729
Elovic	q_m (mg/g)	K_E (L/g)	R^2
	3.7622	0.5911	0.8556
Redlich-Peterson	a_R	K_R (L/g)	R^2
	214.584	8.2564	0.6343

4. Conclusions

The activated carbon annatto peel (ACAP) can be produced from the carbonization process at the temperature of 400°C for an hour and two-stage activation process (physical and chemical) with a 30% H_3PO_4 as an activator and the impregnation ratio of 1:4 (w/w) for 24 hours. The adsorption kinetics of ACAP on annatto seed extract (ASE) followed the pseudo second-order kinetic model with the rate constant of adsorption is 78.5514 g mg⁻¹ h⁻¹ on 150 minutes for contact times. This adsorption process followed the Elovic isotherm model with the assumption of multilayer adsorption.

Acknowledgment

We want to thank the Universitas Kristen Satya Wacana for the financial support through an Hibah Penelitian Internal Skim Penelitian Perseorangan/Kelompok Wajib (Internal Research Grant for Individual/Group Research Scheme) Fiscal Year 2017-2018.

References

- [1] Pari G, Santoso A, Hendra D, Buchari B, Maddu A, Rachmat M, Harsini M, Heryanto T and Darmawan S 2013 Karakterisasi Struktur Nano Karbon Dari Lignosellulosa *Jurnal Penelitian Hasil Hutan* **31** 1 75-91
- [2] Sudaryanto Y, Hartono S, Irawaty W, Hindarso H and Ismadji S 2006 High surface area activated carbon prepared from cassava peel by chemical activation *Bioresour. Technol.* **97** 5 734-9
- [3] Matos J, Nahas C, Rojas L and Rosales M 2011 Synthesis and characterization of activated carbon from sawdust of Algarroba wood. 1. Physical activation and pyrolysis *J. Hazard. Mater.* **196** 360-9
- [4] Giraldo L and Moreno-Piraján J C 2012 Synthesis of activated carbon mesoporous from coffee waste and its application in adsorption zinc and mercury ions from aqueous solution *J. Chem.* **9** 2 938-48
- [5] Chowdhury Z Z, Zain S M, Khan R A and Islam M S 2012 Preparation and characterizations of activated carbon from kenaf fiber for equilibrium adsorption studies of copper from wastewater *Korean J. Chem. Eng.* **29** 9 1187-95
- [6] Salman J 2014 Optimization of preparation conditions for activated carbon from palm oil fronds using response surface methodology on removal of pesticides from aqueous solution *Arab. J. Chem.* **7** 1 101-8
- [7] Kumar A and Jena H M 2016 Preparation and characterization of high surface area activated carbon from Fox nut (*Euryale ferox*) shell by chemical activation with H_3PO_4 *Results Phys.* **6** 651-8

- [8] Melati A and Hidayati E 2016 Synthesis and characterization of carbon nanotube from coconut shells activated carbon *J. Phys. Conf. Ser.* **694** 1 012073
- [9] Shamsuddin M, Yusoff N and Sulaiman M 2016 Synthesis and characterization of activated carbon produced from kenaf core fiber using H₃PO₄ activation *Procedia Chem.* **19** 558-65
- [10] Chen R, Li L, Liu Z, Lu M, Wang C, Li H, Ma W and Wang S 2017 Preparation and characterization of activated carbons from tobacco stem by chemical activation *J. Air Waste Manage. Assoc.* **67** 6 713-24
- [11] Hallagan J, Allen D and Borzelleca J 1995 The safety and regulatory status of food, drug and cosmetics colour additives exempt from certification *Food Chem. Toxicol.* **33** 6 515-28
- [12] Gulrajani M, Gupta D and Gupta P 2003 Application of natural dyes on bleached coir yarn *Indian Journal of Fibre & Textile Research* **28** 466-70
- [13] Das D 2007 Dyeing of wool and silk with Bixa orellana *Indian Journal of Fibre & Textile Research* **32** 366-72
- [14] Selvi A T, Aravindhan R, Madhan B and Rao J R 2013 Studies on the application of natural dye extract from Bixa orellana seeds for dyeing and finishing of leather *Ind. Crops. Prod.* **43** 84-6
- [15] Chuyingsakuntip S and Tangsathitkulchai C 2013 Adsorption of Natural Aluminium Dye Complex from Silk-Dyeing Effluent Using Eucalyptus Wood Activated Carbon *Am. J. Anal. Chem.* **4** 08 379
- [16] Foo K and Hameed B 2012 Preparation, characterization and evaluation of adsorptive properties of orange peel based activated carbon via microwave induced K₂CO₃ activation *Bioresour. Technol.* **104** 679-86
- [17] Zhang Y, Pan K and Zhong Q 2013 Characteristics of activated carbon and carbon nanotubes as adsorbents to remove annatto (norbixin) in cheese whey *J. Agric. Food Chem.* **61** 38 9230-40
- [18] Sastrohamidjojo H 2018 *Dasar-dasar spektroskopi*: UGM PRESS)
- [19] Girgis B S, Temerk Y M, Gadelrab M M and Abdullah I D 2007 X-ray diffraction patterns of activated carbons prepared under various conditions *Carbon Letters* **8** 2 95-100
- [20] Ayawei N, Ebelegi A N and Wankasi D 2017 Modelling and interpretation of adsorption isotherms *J. Chem.* **2017**